

Extensions of Counterion Condensation Theory. 2. Cell Model and Osmotic Pressure of DNA

J. Michael Schurr* and Bryant S. Fujimoto

University of Washington, Department of Chemistry, Box 351700, Seattle, Washington 98195-1700

Received: November 7, 2002; In Final Form: February 11, 2003

In a previous paper, counterion condensation theory was extended by invoking a new alternative auxiliary assumption in order to treat isolated polyions with alternative geometries (beyond a line charge) at finite salt concentrations. Now this theory is further extended to treat a cell model and the osmotic pressures of relatively concentrated DNA solutions in equilibrium with bathing solutions of different salt concentration. Results of the present theory are compared with recently published experimental data of Raspaud et al. and with theoretical calculations of Hansen et al., who combined *zero-salt* solutions of the nonlinear Poisson–Boltzmann equation for a uniformly charged cylinder with the Donnan approximation. Surprisingly good agreement with the experimental data is observed, especially at the higher DNA concentrations. Agreement with the calculations of Hansen et al. is also rather good at the higher DNA concentrations, but at lower DNA concentrations the results of Hansen et al. fall significantly below those of the present theory. This discrepancy is due in part to the fact that polyion screening by the invading salt is omitted in the theory of Hansen et al. The level of overall agreement between the predictions of this extended counterion condensation cell-model theory and either the experimental data or the calculations of Hansen et al. supports the alternative auxiliary assumption that underlies the present theory.

Introduction

Extensive osmotic pressure data for DNA solutions of different concentration in equilibrium with bathing solutions of relatively low ionic strength were recently reported.¹ Both small ions and solvent were equilibrated across the semipermeable membrane. Of particular interest is the regime of moderately high DNA and relatively low salt concentration, where the counterions released by the DNA are expected to dominate its osmotic pressure. Analyses of those data were performed using both counterion condensation theory for a continuous line charge^{2–6} and nonlinear Poisson–Boltzmann theory for a cell model.^{7–9} It was concluded that counterion condensation theory for a line charge^{1,7} gave a rather poor account of the experimental data. In contrast, nonlinear Poisson–Boltzmann theory for a cell model of a uniformly charged cylinder with the diameter d and linear charge density $e/(1.7 \text{ \AA})$ of DNA *in the absence of salt*, together with the Donnan approximation, yielded reasonably good agreement with those same data, except at the lower salt concentrations.⁷ There are several possible reasons for the failure of the line-charge counterion condensation theory to account for such experimental data, and those may be divided into two classes. First, there may be some serious flaw in the fundamental premise of counterion condensation theory, according to which the nonlinear part of the interaction between a polyion and its counterions can be modeled by a quasi-chemical binding equilibrium in a self-consistent manner. Because counterion condensation theory appears to work fairly well in many other regards,^{4–6,10–18} this possibility seems perhaps unlikely. Second, the model of an isolated line charge may be inappropriate for the experimental conditions, which involve (1) rather high counterion concentrations, such that λd is *not* much smaller than 1.0, where λ is the Debye screening parameter and d is the diameter of the array of polyion charges,

and (2) a circumstance wherein uncondensed counterions from the DNA contribute significantly to the total counterion concentration and λ . We recently extended counterion condensation theory to treat alternative geometries besides a line charge at finite salt concentration.¹⁹ In the present work we extend that theory further to treat a cell model, wherein uncondensed counterions from the DNA contribute significantly to the total counterion concentration and λ .

The extension of counterion condensation theory to take account of the actual structure of the array of intrinsic polyion charges at finite salt concentration was proposed, developed, and tested both qualitatively and quantitatively in a paper hereinafter referred to as paper 1.¹⁹ That theory applies to any isolated array of identical charges in electrostatically equivalent locations, including periodic arrays of infinite extent, regular planar polygons, and regular and Archimedian polyhedra. The final formula for the bound, or condensed, fraction of polyion charge (r) is considerably simpler than the original expression of Manning,^{4,5} does not require foreknowledge of the free volume, or equivalently the site binding constant (β'), of the counterions, and is almost trivial to apply. Both r and β' were evaluated over a wide range of concentration for various discrete arrays of infinite extent, namely single charged lines, two parallel charged lines, charged single helices, charged double helices, and a cylindrical array of charged lines designed to model a uniformly charged cylinder. For every long linearly extended geometry *at sufficiently low counterion concentration*, r invariably approaches the value expected for a line charge with the same linear charge density.^{19,20} However, when the product λd becomes comparable to 1.0, the screening of lateral interactions acts to reduce r below its limiting low-salt value. A further reduction of r down to zero occurs when $\lambda b > 1.0$, where b is the longitudinal spacing of intrinsic charges along the axis of the polyion. Thus, r is expected to decline below its

limiting value, even for a discretely charged line, when λb is no longer negligibly small compared to 1.0.¹⁹

This extended counterion condensation (ECC) theory was applied to a uniformly charged cylinder with the diameter $d = 20$ Å and linear charge density $e/(1.7$ Å) of DNA, where e is the electronic charge.¹⁹ The predicted condensed fractions, r , were compared with those obtained from nonlinear Poisson–Boltzmann (NLPB) theory over a wide range of uni-univalent salt concentration. In our interpretation, the condensed counterion charge is simply the difference between the actual polyion charge and the effective charge that enables the solution of the linearized Poisson–Boltzmann (LPB) equation to precisely match that of the NLPB equation in the “linear” tail region of the latter. For a uniformly charged cylinder, $r = (\nu_{\text{act}} - \nu_{\text{eff}})/\nu_{\text{act}}$, where ν_{act} and ν_{eff} are, respectively, the actual and effective charges per unit length. Results from the ECC theory agree closely with those from the NLPB theory for isolated polyions at low salt concentrations (≤ 0.0003 M) and again at 0.1 M and deviate only modestly ($\leq 15\%$) over the entire range from 0.0003 to 0.15 M.¹⁹ Over this latter range, λd increases from 0.11 to 2.54, and the lateral interactions between opposite sides of the cylinder become significantly screened. As a consequence, the r -values predicted by both theories decrease from near 0.76, characteristic of a line charge, in 0.0003 M salt to 0.47 in 0.1 M salt. The findings in part 1 collectively suggest that counterion condensation theory may provide a quantitatively useful approximation, when properly extended to account for the actual geometry of the polyion and the prevailing finite salt concentration.

The present interpretation of the condensed fraction is somewhat unconventional but may perhaps provide the most relevant comparison between nonlinear Poisson–Boltzmann theory and counterion condensation theory, since the latter takes no account of the structure of the condensed ion “cloud” or inner ion atmosphere. The quantity $(1 - r)N|e|$ is simply the effective polyion charge inferred from the magnitude of the electrostatic potential in its linear region at great distances by using the linear theory appropriate for the geometry in question.

The ECC theory rests upon a plausible, but as yet unfounded, auxiliary assumption regarding the coupled variation of the condensed fraction, r , of counterion charge and the counterion site binding constant, β' , or equivalently the free volume, with counterion concentration (m_{C}).¹⁹ Its approximate validity and utility are ultimately to be determined by comparing results of the ECC theory with those of more exact theories, such as NLPB theory, and with relevant experimental data, as will be done here. We note that all previous protocols for extending counterion condensation theory to finite salt concentration invoked a different auxiliary assumption, namely $\partial\beta'/\partial m_{\text{C}} = 0$ for all m_{C} , which is similarly unfounded but also is incorrect and leads to qualitatively incorrect predictions for the variation of r with m_{C} , as demonstrated in detail in part 1.¹⁹ Our work on counterion condensation theory is not intended to supplant NLPB theory with a more approximate and less well founded theory in any circumstance wherein the former can reasonably be applied. Instead, we are investigating the accuracy and limitations of a simple ECC protocol that may provide quantitatively useful approximate r -values for polyions of arbitrary and complex structure, for which the NLPB theory cannot yet reasonably be applied. The simplicity of counterion condensation theory stems from its use of linear Debye–Hückel potentials (*after* accounting for counterion condensation), which can be linearly superposed.

The previously formulated ECC theory¹⁹ pertains to an isolated polyion in an infinite salt reservoir, wherein the

concentration of free counterions is unaffected by the fraction of uncondensed counterions, $1 - r$. Consequently, that version of ECC theory would not be expected to apply to the relevant experimental data of Raspaud et al.¹ In that case, an electro-neutral cell model is more appropriate.

Our principal objectives in this paper are as follows. First, a version of ECC theory appropriate for an electroneutral cell model is developed. This is then applied along with the Donnan approximation to calculate the osmotic coefficient ϕ . ϕ is defined as the ratio of the osmotic pressure of the polyion solution in ionic equilibrium with a bathing salt solution to that expected for an ideal gas of all the counterions that are either associated with, or derived from, the polyion (excluding any Donnan or other contribution from the neutral salt). Results of this ECC cell-model (ECCC) theory are then compared with the relevant experimental data¹ and with the corresponding calculations of Hansen et al.,⁷ who combined the cell-model solution of the NLPB equation in zero salt with the Donnan approximation.

Counterion Condensation Theory for a Cell Model

We consider a solution of *highly charged* polyions that is separated from a solution of uni-univalent salt by a membrane that is permeable to both the solvent and the small ions. When the concentration of polyion charge greatly exceeds the salt concentration, the osmotic pressure of the polyion solution relative to that of its bathing salt solution exceeds by *very many fold* the value expected for the corresponding *neutral* polyion. Under such conditions, the *ideal* contribution of the polyions per se to the osmotic pressure is negligible, and their nonideal contribution can be attributed primarily to the small counterions and coions within the polyion chamber. When the salt concentration is sufficiently low and the polyion concentration sufficiently high, rodlike polyions begin to adopt parallel configurations²¹ that may locally resemble a hexagonal array. We associate with each polyion rod a concentric cylindrical cell, whose radius R is chosen such that the sum of cell volumes equals the total volume of the polyion solution.^{7–9,22–24} The contents of each cell are assumed to be electrically neutral. Consequently, each polyion does not interact electrostatically with either polyions or small ions in adjacent cells but instead interacts only with itself, its uncondensed counterions, and any salt ions within its own cell. In this cell model picture the interactions between polyions arise indirectly from the confinement of those counterions that compensate the polyion charge within the finite cell and from the concomitant Donnan exclusion of the bathing salt. These are the factors that determine the very large osmotic pressure, which reflects a very large increase in free energy with decreasing volume of the polyion chamber or equivalently with decreasing distance between polyions. The outer boundary of the cell at a distance $x = R$ from the center of the cylinder is assumed to be sufficiently far from the outer charges of the polyion that the electrostatic potential in the vicinity of R exhibits no significant longitudinal corrugations with distance z along the symmetry axis, despite the periodic distribution of intrinsic charges along the polyion. Hence, the electrostatic potential gradient at large distances from the axis is normal to the outer boundary. Moreover, according to Gauss’s law, that normal electric field is expected to vanish everywhere over the cell boundary at R . By convention, the electrostatic potential is also assigned the value zero at R . In this work the small counterions and coions are assumed to be *univalent*, as are also the intrinsic charges of the polyion. The *molar* concentration of the uncondensed or unbound counterions at $x = R$ is denoted by m_{C}^{R} , and the average concentration of

uncondensed counterions throughout the cell is denoted by \bar{m}_C . The concentration of coions at $x = R$ is denoted by m_b^R , and the average concentration of coions throughout the cell is denoted by \bar{m}_b . The salt concentration at any position x in the cell is taken to be that of the coions, that is $m_s(x) = m_b(x)$. Thus, the salt concentration at R is $m_s^R = m_b^R$ and the average salt concentration throughout the cell is $\bar{m}_s = \bar{m}_b$. The counterion conservation condition, which derives from the requirement of overall cell neutrality, is given by

$$\bar{m}_C = m_1(1 - r) + \bar{m}_s \quad (1)$$

where m_1 is the concentration of intrinsic polyanion charges and r is the condensed fraction of counterions. Each polyanion is assumed to comprise a large number N of geometrically and electrostatically equivalent intrinsic charges. The condensed fraction is

$$r = n_C/N \quad (2)$$

where n_C is the average number of bound, or condensed, counterions on the polyanion. In counterion condensation theory, the uncondensed counterions and coions at any distance x from the cell center are assumed to experience only the linear, or Debye–Hückel, part ($\psi^{\text{DH}}(x)$) of the total electrostatic potential. Provided that x is sufficiently large, $\psi^{\text{DH}}(x)$ will be sufficiently small that $u(x) \equiv |e\psi^{\text{DH}}(x)|/kT \ll 1.0$, where k is Boltzmann's constant and T is the absolute temperature. Under these low potential conditions

$$m_j(x) = m_j^R e^{-z_j u(x)} \cong m_j^R \quad (3)$$

where $j = C$ or b denotes counterions or coions and z denotes the ion valence. Provided that the distance, $R - d/2$, between the outer cell boundary and the polyanion radius ($d/2$) is sufficiently large that $\exp[-\lambda(R - d/2)] \ll 1.0$, as assumed here, the small-potential condition will be obeyed over almost the entire volume of the cell. This circumstance is favored by the fact that the volume of a cylindrical shell from x to $x + dx$ increases in proportion to x and reaches its maximum at $x = R$. Thus, in computing $\bar{m}_C \equiv \langle m_C(x) \rangle$ and $\bar{m}_s \equiv \langle m_s(x) \rangle$, the regions of largest x are weighted most heavily. Under these conditions, we can approximate

$$\bar{m}_s = \langle m_s(x) \rangle = \langle m_b(x) \rangle = m_b^R \langle e^{-z_b u(x)} \rangle \cong m_b^R = m_s^R \quad (4)$$

and from eqs 1 and 4,

$$\bar{m}_C \cong m_1(1 - r) + m_s^R = m_C^R \quad (5)$$

The Debye screening parameter is $\lambda \equiv (4\pi L_B(N_A/1000)(\bar{m}_C + \bar{m}_s))^{1/2}$, where $L_B = e^2/\epsilon kT$ is the Bjerrum length, ϵ is the dielectric constant, k is Boltzmann's constant, and T is the absolute temperature. Using eqs 4 and 5, λ can be approximated by

$$\lambda = (4\pi L_B(N_A/1000)(m_1(1 - r) + 2m_s^R))^{1/2} \quad (6)$$

The total chemical potential (i.e. electrochemical potential) of an uncondensed counterion anywhere in the cell must be given by

$$\mu_C = \mu_C^\circ + kT \ln(m_C^R/m_0) \quad (7)$$

where $m_0 = 55.6$ and μ_C° is the chemical potential of a counterion in its mole fraction 1.0 standard state. Equation 7

applies because (i) the electrostatic potential vanishes at R and (ii) the chemical potential must be the same everywhere throughout the cell at equilibrium. Similarly, for the coions anywhere in the cell,

$$\mu_b = \mu_b^\circ + kT \ln(m_b^R/m_0) \quad (8)$$

The derivation of the binding isotherm relation is described briefly in the Appendix. This development follows that in Appendix A of part 1 and leads to eq A9 in the Appendix of this paper. The application of the auxiliary condition in this case requires additional considerations that are also described in the Appendix. The final result in eq A19 can be expressed in a slightly more convenient manner by using eq A20 to obtain

$$r = 1 -$$

$$\frac{1}{(m_C^R)^{1/2} L_B K \left(\frac{m_{si}^R}{2m_C^R} \right)^{1/2} \left\{ -\frac{\partial S}{\partial \lambda} \left(1 + \frac{m_1(1-r)}{4m_{si}^R} \right) - \left(\frac{m_1(1-r)}{4m_{si}^R} \right) \lambda \frac{\partial^2 S}{\partial \lambda^2} \right\}} \quad (9)$$

where $m_{si}^R \equiv m_C^R + m_b^R = m_1(1 - r) + 2m_s^R$ is the total concentration of small ions at the outer cell boundary and $S(\lambda)$ is the interaction sum in eq A5. This cell model expression for r differs from the corresponding expression for an isolated polyanion in an infinite salt reservoir in three respects: (1) m_C has been replaced everywhere by m_C^R at the outer cell boundary; (2) the factor $(m_{si}^R/2m_C^R)^{1/2}$ now appears; (3) the terms containing the factor $m_1(1 - r)/(4m_{si}^R)$ now appear. The latter two modifications arise from the counterion conservation condition. For an isolated polyanion in an infinite salt reservoir, $m_1(1 - r)/m_s^R \rightarrow 0$, so $m_{si}^R/(2m_C^R) \cong 2m_s^R/(2m_s^R) = 1.0$ and $m_1(1 - r)/m_{si}^R \cong m_1(1 - r)/(2m_s^R) \rightarrow 0$. In that case, the $(m_{si}^R/2m_C^R)^{1/2}$ factor becomes 1.0, the terms containing $m_1(1 - r)/m_{si}^R$ vanish, and eq 9 for r becomes identical to that obtained previously for an isolated polyanion in an infinite salt reservoir.¹⁹

The Donnan Approximation

When the counterions and coions in the cell are in osmotic equilibrium with salt at concentration m_s° in the bathing solution, their respective total chemical (i.e. electrochemical) potentials in the cell must match the corresponding values in the bathing solution. The electrostatic potential at the cell boundary ($\psi(R) = 0$) relative to that of the bathing solution (ψ^{BS}) is $\psi^{\text{rel}}(R) = 0 - \psi^{\text{BS}}$, and the corresponding reduced potential at the cell boundary relative to that of the bathing solution is denoted by $u_0 \equiv |e|\psi^{\text{rel}}(R)/kT$. The corresponding chemical potentials of the counterions and coions at the cell boundary are then given by

$$\mu_C^R = \mu_C^{\text{BS}} + z_C kT u_0 = \mu_C^\circ + kT \ln m_s^\circ + z_C kT u_0 \quad (10a)$$

$$\mu_b^R = \mu_b^{\text{BS}} + z_b kT u_0 = \mu_b^\circ + kT \ln m_s^\circ + z_b kT u_0 \quad (10b)$$

Combining eqs 7 and 8 with eqs 10a and 10b and noting that $z_b = -z_C$ yields

$$m_C^R m_b^R = m_s^{\circ 2} \quad (11)$$

After inserting eq 5 into eq 11, using $m_b^R = m_s^R$, and solving for m_s^R , we obtain

$$m_s^R = m_s^o \left(\left(1 + \left(\frac{m_1(1-r)}{2m_s^o} \right)^2 \right)^{1/2} - \frac{m_1(1-r)}{2m_s^o} \right) \quad (12)$$

Using eq 11 in eqs 5 and A20 yields also

$$m_C^R = m_1(1-r) + m_s^o \left(\left(1 + \left(\frac{m_1(1-r)}{2m_s^o} \right)^2 \right)^{1/2} - \frac{m_1(1-r)}{2m_s^o} \right) \quad (13a)$$

$$m_{si}^R = m_1(1-r) + 2m_s^o \left(\left(1 + \left(\frac{m_1(1-r)}{2m_s^o} \right)^2 \right)^{1/2} - \frac{m_1(1-r)}{2m_s^o} \right) \quad (13b)$$

After eqs 12, 13a, and 13b are employed in eqs 6 for λ and 9 for r , the entire right hand side of eq 9 depends only upon $m_1(1-r)$ and m_s^o and known physical and geometrical constants. With m_1 and m_s^o fixed at the known experimental values, eq 9 can be easily solved for r by iteration. An important aspect of this protocol is that the Donnan condition in eq 12 is automatically taken into account on every step of the iteration.

The Osmotic Pressure

Because the Maxwell stress vanishes at the outer cell boundary, the osmotic pressure of the cell-model polyion solution (π_p) relative to that of pure solvent arises entirely from the uncondensed counterions and coions at R .⁷ That is,

$$\pi_p = kT(N_A/1000)(m_{si}^R)(0.1) \quad (14)$$

where 0.1 is the factor required to convert from cgs to mks (SI) units. The osmotic pressure of the cell-model polyion solution relative to that of the bathing solution (π_s) is then given by

$$\pi_p - \pi_s = kT(N_A/1000)(m_{si}^R - 2m_s^o)(0.1) \quad (15)$$

By definition, the osmotic coefficient is then

$$\phi = \frac{m_{si}^R - 2m_s^o}{m_1} \quad (16)$$

Calculations of ϕ were carried out for a double-helical array of discrete charges. This array is formed in the following way. A single-helix with radius $R = 11$ Å has 10 regularly spaced electronic charges per turn, such that the longitudinal spacing between charges in a direction parallel to the symmetry axis is $h = 3.4$ Å. The second helix of the double-helix is obtained by rotating a helix that is initially coincident with the first helix by π rad around the symmetry axis. The double helix then has 20 charges per turn. The computed osmotic coefficients are weakly sensitive to the radius of the charge array, which in the case of DNA is believed to be about 11 Å. Other parameters of the calculation are taken to be temperature, $T = 298$ K, and relative dielectric constant, $\epsilon = 78$, which gives $L_B = 7.18 \times 10^{-8}$ cm. The sums in eq 9 are evaluated directly using

$$-\frac{\partial S}{\partial \lambda} = \sum_{j=1}^{1000} e^{-\lambda R_{oj}^{(1)}} + \frac{1}{2} e^{-\lambda 2R} + \sum_{j=1}^{1000} e^{-\lambda R_{oj}^{(2)}} \quad (17)$$

and

$$\frac{\partial^2 S}{\partial \lambda^2} = \sum_{j=1}^{1000} R_{oj}^{(1)} e^{-\lambda R_{oj}^{(1)}} + R e^{-\lambda 2R} + \sum_{j=1}^{1000} R_{oj}^{(2)} e^{-\lambda R_{oj}^{(2)}} \quad (18)$$

where

$$R_{oj}^{(1)} = ((jh)^2 + (2R \sin(j\phi_0/2))^2)^{1/2} \quad (19)$$

is the distance from a given charge (the 0th) to the j th charge in one direction along the same single-helix and

$$R_{oj}^{(2)} = ((jh)^2 + R^2(\cos(j\phi_0 + \pi) - 1)^2 + R^2(\sin(j\phi_0))^2)^{1/2} \quad (20)$$

is the distance from the 0th charge to the j th charge in one direction along the opposite helix. The succession angle of the helix is $\phi_0 = 2\pi/10$. Summing to the 1000th distant charge provides satisfactory convergence of the sums under the conditions investigated here.

The calculation is performed by using Mathematica 4.0 running on a Pentium Pro processor. Equation 12 for m_s^R is incorporated symbolically into eq 6 for λ , which in turn is incorporated symbolically into eqs 17 and 18 for $(-\partial S/\partial \lambda)$ and $\partial^2 S/\partial \lambda^2$, which are then substituted symbolically into eq 9 for r . Equations 13a and 13b for m_C^R and m_{si}^R are similarly substituted symbolically into eq 9, whose right hand side now depends only on the fixed values of m_1 and m_s^o , known physical and geometrical constants, and the unknown value of r . A suitable trial value of r , such as the limiting value for the isolated polyion in an infinite zero-salt reservoir, is adopted, and eq 9 is then solved by iteration for the “stationary” value of r by using the FixedPoint command. The number of iterations required for satisfactory convergence is determined by using the NestList command and was generally found to be less than 15 and usually less than 10. The resulting value of r is then used in eq 13b to determine m_{si}^R , which is finally inserted into eq 16 to obtain ϕ . The typical running time, with 20 iterations in both NestList and FixedPoint commands, was about 20 ss to calculate each value of r and ϕ for a given set of conditions.

Results and Discussion

In Figure 1, the osmotic coefficients predicted by the ECCC theory via eqs 9 and 16 are plotted versus $\log_{10}(C_p)$, where $C_p \equiv m_1$ is the molar DNA phosphate concentration. The solid line applies for a bathing solution of 2 mM salt, and the dashed line applies for 10 mM salt. The solid circles and squares are the experimental data of Raspaud et al.¹¹ for the 2 and 10 mM salt bathing solutions, respectively. In the case of the 2 mM salt bathing solution, agreement between the ECCC theory and experiment is fairly good over the entire C_p -range of the measured data. In the case of the 10 mM salt bathing solution, agreement is good from $C_p = 0.276$ M ($\log_{10}(0.276) = -0.56$) down to 0.08 M ($\log_{10}(0.08) = -1.10$), but from $C_p = 0.066$ M ($\log_{10}(0.066) = -1.18$) to 0.005 M ($\log_{10}(0.005) = -2.3$) the predictions of the ECCC theory substantially exceed the experimental data. At still lower $C_p \lesssim 0.002$ M ($\log_{10}(0.002) = -2.7$) the predicted ϕ values significantly underestimate the experimental values. In any case, the overall agreement of the ECCC predictions with the experiments suffices to demonstrate that the alternative auxiliary assumption in eq A14, upon which the ECCC theory rests, provides a quantitatively useful approximation, especially at the higher polyion concentrations.

A principal objective of the experiments was to measure osmotic coefficients in the regime of high C_p and low m_s^o , wherein the osmotic coefficient is expected to approach the unbound fraction $1-r$. It is instructive to compare the ECCC predictions for both ϕ and $1-r$ at different C_p . For the 0.002 M salt bathing solution, the ratio $\phi/(1-r)$ descends from 0.995 at $C_p = 0.26$ M to 0.75 at $C_p = 0.06$ M, and further to 0.35 at

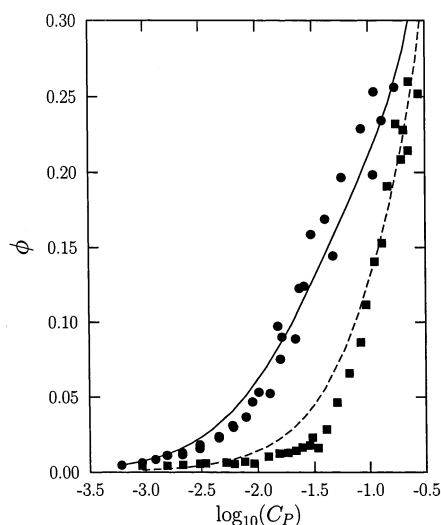


Figure 1. Osmotic coefficient ϕ of DNA vs $\log_{10}(C_p)$, where C_p is the molar concentration of intrinsic polyanion charges. The symbols are experimental data of Raspaud et al.¹ The curves are computed according to the extended counterion condensation cell-model (ECCC) theory embodied in eqs 6, 9, 11–13b, and 16, as described in the text. The model DNA is a symmetrical double-helical array of discrete univalent charges of diameter $d = 22$ Å with an axial spacing 3.4 Å between pairs of charges (one on each single-helix). The filled circles (●) and solid line apply for a bathing solution of 2 mM salt, and the filled squares (■) and dashed line apply for 10 mM salt.

$C_p = 0.015$ M, and continues to descend at lower C_p . In this case, the ratio $\phi/(1-r)$ is nearly 1.0 at the highest C_p examined and remains above 0.75 for C_p down to 0.06 M. Thus, the approximately twofold decrease in ϕ over this same range ($C_p = 0.26$ to 0.06 M) is due primarily to a decrease in $1-r$, or equivalently an increase in r , which in turn is caused by diminished screening as C_p decreases. For the 0.01 M salt bathing solution, the ratio $\phi/(1-r)$ descends from 0.80 at $C_p = 0.26$ M to 0.33 at $C_p = 0.06$ M, and further to 0.089 at $C_p = 0.015$ M, and continues to descend at lower C_p . Thus, in the case of the 0.01 M salt bathing solution, the ratio $\phi/(1-r)$ reaches no higher than 0.80 at the highest C_p examined and descends rather quickly to much lower values.

Agreement of the present ECCC theory with the experimental data is very similar to that exhibited by the calculations of Hansen et al.⁷ Those authors used the *zero-salt* cell-model solution of the nonlinear Poisson–Boltzmann equation for a uniformly charged cylinder with radius $d/2 = 12$ Å and the linear charge density of DNA, and they invoked the same Donnan assumption employed in the ECCC theory. Their calculated ϕ -values agree well with the experimental data at high C_p for both the 0.002 and 0.01 M salt bathing solutions. For the 0.002 M salt bathing solution, their calculated ϕ -values significantly underestimate the experimental data for all $C_p \lesssim 0.01$ M. For the 0.01 M salt bathing solution, their calculated ϕ -values significantly exceed the experimental data between $C_p = 0.066$ and 0.02 M, and then they significantly underestimate the experimental data for $C_p \lesssim 0.005$ M. The differences between the two theories in regard to quality of the fits in the region of low C_p , namely $C_p \lesssim 0.066$ M for the 0.01 M salt bathing solution and $C_p \lesssim 0.01$ M for the 0.002 M bathing solution, all stem from the fact that the calculated ϕ -values of Hansen et al. significantly underlie the ϕ -values predicted by the ECCC theory in that region, as discussed below.

The predicted osmotic coefficients of the ECCC theory (ϕ_{ECCC}) are compared with those of Hansen et al. (ϕ_{NLPB}) by computing the ratio $\phi_{\text{ECCC}}/\phi_{\text{NLPB}}$ and plotting that versus \log_{10} -

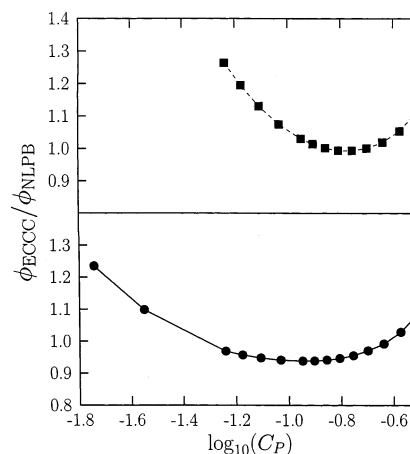


Figure 2. Ratio $\phi_{\text{ECCC}}/\phi_{\text{NLPB}}$ vs $\log_{10}(C_p)$, where C_p is the molar concentration of intrinsic polyanion charges. The ϕ_{NLPB} values were computed by Hansen et al.,⁷ who combined the zero-salt solution of the nonlinear Poisson–Boltzmann equation with the Donnan approximation. The ϕ_{ECCC} values are results of the extended counterion condensation cell-model theory, embodied in eqs 6, 9, 11–13b, and 16. The NLPB solution applies for an impermeable, uniformly charged cylinder of diameter $d = 24$ Å with the linear charge density of DNA. The ϕ_{ECCC} results apply for a permeable symmetrical double-helical array of charges with the same diameter $d = 24$ Å and linear charge density. The bathing salt solution is 10 mM for the top panel and 2 mM for the bottom panel.

(C_p), as illustrated in Figure 2. In this case (only), ϕ_{ECCC} is calculated for a double-helix of radius $d/2 = 12$ Å, chosen to match that of the uniformly charged cylinder treated by Hansen et al.⁷ For the 0.002 M salt bathing solution, we find that $0.90 \leq \phi_{\text{ECCC}}/\phi_{\text{NLPB}} \leq 1.10$ for C_p in the range 0.31–0.018 M, and with further decreases in C_p , this ratio rises monotonically. For the 0.01 M salt bathing solution, we find that $0.90 \leq \phi_{\text{ECCC}}/\phi_{\text{NLPB}} \leq 1.10$ for C_p in the range 0.31–0.058 M, and with further decreases in C_p , this ratio rises monotonically. The substantial and increasing disagreement between ϕ_{ECCC} and ϕ_{NLPB} with decreasing C_p in the low C_p range is at first glance puzzling, because the cell-model assumptions of the ECCC theory should improve with increasing cell size (caused by decreasing C_p), and the ECCC condensed fractions r should approach those expected for an isolated polyanion in 0.002 or 0.01 M salt solution. The latter r -values were previously found to differ by less than 15% from the corresponding r -values obtained by numerically solving the nonlinear Poisson–Boltzmann equation for the same *isolated* uniformly charged cylinder over the same range of salt concentration. We suspect that the much larger discrepancy found at low polyanion concentration in this case is due to the failure of an assumption invoked by Hansen et al.,⁷ namely that the contribution of the invading salt to the screening can be ignored, as described further below.

In the cases of both the 0.002 and 0.01 M salt bathing solutions, the rise of $\phi_{\text{ECCC}}/\phi_{\text{NLPB}}$ above 1.0 with decreasing C_p is associated with an increase in the fraction, $f_R = 2m_s^R/(m_1(1-r) + 2m_s^R)$, of total small-ions at R that belong to the invading salt, specifically an increase of this fraction to values greater than 0.3 to 0.4. That is, when the small-ions from the salt become significant compared to the uncondensed counterions from the polyanion, the ratio $\phi_{\text{ECCC}}/\phi_{\text{NLPB}}$ begins to rise. In the ECCC theory, the effect of the invading salt is to increase the screening and consequently diminish the value of r somewhat, which thereby releases more condensed ions and elevates ϕ_{ECCC} over what it would be in the absence of invading salt. However, the corresponding effect is prohibited in the

calculations of Hansen et al., who used always the *zero-salt* solutions of the nonlinear Poisson–Boltzmann equation. All of the screening in their treatment comes from the polyion-associated counterions (both “free” and “condensed”), and none derives from the salt. As they note, this assumption is expected to hold when C_p is sufficiently large and the invading salt concentration is sufficiently low, but it is expected fail when C_p is too low. The ECCC results suggest that this mode of failure becomes significant when $f_R \cong 0.3$ – 0.4 and steadily worsens with decreasing salt concentration. Hence, we suspect that the ϕ_{NLPB} values of Hansen et al. are significantly lower than the value that would have been obtained by allowing the invading salt to contribute to the screening in the regime $C_p \lesssim 0.018$ M in the case of the 0.002 M salt bathing solution and in the regime $C_p \lesssim 0.058$ M in the case of the 0.01 M bathing solution. Therefore, we suggest that the rise of the ratio, $\phi_{\text{ECCC}}/\phi_{\text{NLPB}}$, above 1.0 in the low salt regime is due at least in part to a downward error in ϕ_{NLPB} that arises from the zero-salt assumption. Investigation of this point via numerical solutions of the NLPB equation in the presence of the invading salt is a topic for future work.

A puzzling feature of the comparison of either theory with experiment is the cutting of the “corner” of the experimental data for the 0.01 M bathing solution over the range $0.02 \leq C_p \leq 0.066$ by both theories. Although the discrepancy is significantly greater for ϕ_{ECCC} than for ϕ_{NLPB} , that difference might simply reflect the downward error in ϕ_{NLPB} discussed above. The cell diameter is $2R = 137$ Å at $C_p = 0.066$ M and $2R = 249$ Å at $C_p = 0.02$ M. The experimental osmotic pressure could conceivably be diminished by a component of interpolyion attractive forces due to correlated charge fluctuations. Though not so large as to cause net attraction, they could conceivably reduce the net repulsion. Although such charge fluctuation forces probably have too short a range to be significant at the mean inter-polyion distance ($\sim 2R$), they could conceivably promote fluctuations in which certain pairs of duplex strands moved considerably closer than the mean distance. Whatever is the ultimate explanation, it is noteworthy that the experimental osmotic pressure significantly underlies the predictions of both theories in this range of C_p (0.066–0.020 M) in the case of the 0.01 M salt bathing solution but not in the case of the 0.002 M salt bathing solution, where the net effective repulsions between polyions are much stronger.

Conclusions

The present work demonstrates that the ECCC theory can provide quantitatively useful estimates of the osmotic coefficients of relatively concentrated DNA solutions. This substantially justifies the assumptions upon which the ECCC theory rests, in particular the alternative auxiliary assumption in eq A14. In all, four main features of the model and theory are responsible for the surprisingly good agreement between the ECCC theory and either the experimental data or the theoretical results of Hansen et al. (1) The array of polyion charges has the appropriate radius, $d/2$, unlike a line charge. (2) The alternative auxiliary assumption, eq A14, is invoked. (3) The uncondensed counterions contribute significantly to self-screening of the polyion. (4) The ECCC theory treats a cell model of the DNA solution. The first two features cause a decline of the condensed fraction, or release of condensed counterions, with increasing screening in the regime where $\lambda d/2 \gtrsim 1.0$. The third feature couples increased screening to counterion release, which can significantly decrease the condensed fraction at sufficiently

high ionic strength. The fourth feature, namely the cell model, provides the simplest way to treat the effects of interpolyion interactions, specifically by confining each polyion to an electroneutral cell with a vanishing electric field at the outer cell boundary, and also provides the simplest route to the osmotic pressure, when the bathing solution contains a moderate salt concentration.

Acknowledgment. This work was supported in part by NSF Grant MCB-9982735 from the National Science Foundation. We also wish to thank Dr. P. L. Hansen for supplying both the experimental data of Raspaud et al.¹ and the computed ϕ -values of Hansen et al.⁷

Appendix. Counterion Condensation Theory for a Cell Model of Long Rodlike Polyions

The description of the cell model, definitions of the important quantities, discussion of the approximations involved, and the important starting relations are presented in the section Counterion Condensation Theory for a Cell Model in the text and in eqs 1–7. The binding theory now proceeds exactly as described in Appendix A of part 1, but with m_C^R in place of m_C , up to the first line of eq A15 of part 1, which becomes

$$0 = \frac{\partial}{\partial \bar{n}_C} \left[\bar{n}_C \ln \left(\frac{m_C^R \beta}{m_0} \right) - (A^{\text{el}}(\bar{n}_C) - A^{\text{el}}(0))/kT + \bar{n}_C \ln(N/\bar{n}_C) \right] \quad (\text{A1})$$

$A^{\text{el}}(\bar{n}_C)$ is the electrostatic energy of a polyion with \bar{n}_C bound counterions, and β is the site binding constant for the mole fraction 1.0 standard state. Equation A1 is the condition for the maximum term in the “grand” partition function for the complex. In the case of the cell model, the derivative must be taken subject to the counterion conservation condition, which is imposed by inserting eq 5 for m_C^R into the first term in eq A1 and eq 6 for λ into the second term, which generally depends upon λ , and then making use of eq 2. Taking the indicated derivative now yields

$$0 = \ln \left(\frac{m_C^R \beta}{m_0} \right) - \frac{\bar{n}_C m_1}{m_C^R N} - \frac{\partial A^{\text{el}}(\bar{n}_C)/kT}{\partial \bar{n}_C} + \ln \left(\frac{N}{\bar{n}_C} \right) - 1 \quad (\text{A2})$$

After exponentiating eq A2 and multiplying both sides by $r = \bar{n}_C/N$, there results

$$r = m_C^R \beta' e^{-1} \exp \left[- \frac{\partial A^{\text{el}}(\bar{n}_C)/kT}{\partial \bar{n}_C} \right] \exp \left[- \frac{m_1 r}{m_C^R} \right] \quad (\text{A3})$$

where $\beta' = \beta/m_0$ is the site binding constant for the 1.0 M standard state. As in part 1, we assume that

$$A^{\text{el}}(\bar{n}_C)/kT = (1 - r)^2 L_B N S(\lambda) \quad (\text{A4})$$

wherein the interaction sum ($S(\lambda)$) is defined by

$$S(\lambda) \equiv \frac{1}{2} \sum_{i \neq j}^N e^{-\lambda r_{ij}/r_{jl}} \quad (\text{A5})$$

λ is the Debye screening parameter given in eq 6, and r_{jl} is the distance between the j th and l th intrinsic polyion charges. It is assumed in eq A5 that all intrinsic polyion charges are geometrically equivalent. It is also implicitly assumed that the

distance $R - d/2$ is sufficiently great that the perturbation of the linear Debye–Hückel potential surrounding any given intrinsic polyion charge by the boundary at R is negligibly small. Taking the derivatives as $\partial/\partial\bar{n}_C = (\partial r/\partial\bar{n}_C) \partial/\partial r = (\partial r/\bar{n}_C)(\partial\lambda/\partial r) \partial/\partial\lambda$ and using

$$\frac{d\lambda}{dr} = -(1/2)\lambda 4\pi L_B(N_A/1000)m_1 \quad (\text{A6})$$

yields eventually

$$\exp\left[-\frac{\partial A^{\text{el}}/kT}{\partial\bar{n}_C}\right] = \exp[2(1-r)L_B S(\lambda)] \exp\left[(1-r)^2 L_B \frac{K^2}{4} m_1 \frac{1}{\lambda} \frac{\partial S}{\partial\lambda}\right] \quad (\text{A7})$$

where

$$K \equiv (8\pi L_B N_A/1000)^{1/2} \quad (\text{A8})$$

Substituting eq A7 into A3 yields

$$r = m_C^R \beta' e^{-1} E_1 E_2 E_3 \quad (\text{A9})$$

where

$$E_1 \equiv \exp[2(1-r)L_B S(\lambda)] \quad (\text{A10a})$$

$$E_2 \equiv \exp\left[(1-r)L_B \frac{K^2}{4} m_1 (1-r) \frac{1}{\lambda} \frac{\partial S}{\partial\lambda}\right] \quad (\text{A10b})$$

$$E_3 = \exp\left[-r\left(\frac{m_1}{m_1(1-r) + m_s^R}\right)\right] \quad (\text{A10c})$$

As in part 1, we define the difference function

$$\Delta(r, \beta', m_C^R) = r - m_C^R \beta' e^{-1} E_1 E_2 E_3 \quad (\text{A11})$$

and apply the auxiliary condition

$$(\partial\Delta/\partial m_C^R)_{r, \beta'} = 0 \quad (\text{A12})$$

In the presence of salt, m_C^R can vary at constant r and β' either by varying m_1 (concentration of intrinsic polyion charge) or by varying m_s^R . However, these two possibilities affect λ differently, since the slope of λ with respect to m_1 is lower than the slope of λ with respect to m_s^R by the ratio $(1-r)/2$. Therefore, we take the slope of λ with respect to m_C^R in the following way. The fractions of counterions coming from the first and second terms in eq 5, corresponding to the polyion and salt, are respectively

$$f_1 = m_1(1-r)/m_C^R, \quad f_s = m_s^R/m_C^R \quad (\text{A13})$$

and $f_1 + f_s = 1.0$. We now propose the constraint that f_1 and f_s should remain constant as the auxiliary condition is applied; hence,

$$(\partial\Delta/\partial m_C^R)_{r, \beta', f_1} = 0 \quad (\text{A14})$$

The idea here is to impose the auxiliary condition, namely that Δ be invariant to small changes in m_C , while retaining the

prevailing f_1/f_s ratio. Then we set

$$\begin{aligned} \left(\frac{\partial\lambda}{\partial m_C^R}\right)_{r, \beta', f_1} &= f_1 \frac{\partial\lambda}{\partial(m_1(1-r))} + f_s \frac{\partial\lambda}{\partial m_s^R} \\ &= \frac{1}{2\lambda} \left(\frac{m_1(1-r)}{m_C^R} \frac{K^2}{2} + \frac{m_s^R}{m_C^R} \frac{K^2}{2} \times 2 \right) \\ &= \lambda/2m_C^R \\ &= \frac{1}{2} \frac{K}{2^{1/2}} (m_1(1-r) + 2m_s^R)^{1/2} \frac{1}{m_C^R} \\ &= \frac{1}{2} K \left(\frac{1+f_s}{2} \right)^{1/2} \frac{1}{(m_C^R)^{1/2}} \end{aligned} \quad (\text{A15})$$

and

$$\left(\frac{\partial m_1(1-r)}{\partial m_C^R}\right)_{r, \beta', f_1} = f_1 \frac{\partial m_1(1-r)}{\partial m_1(1-r)} + f_s \frac{\partial m_1(1-r)}{\partial m_s^R} = f_1 \quad (\text{A16})$$

since $\partial(m_1(1-r))/\partial m_s^R$ vanishes when f_1 is held constant. The exponent of the function E_3 can be written as

$$-r \left(\frac{m_1}{m_1(1-r) + m_s^R} \right) = -\frac{r}{1-r} f_1 \quad (\text{A17})$$

which is independent of m_C^R , when r and f_1 are held constant. There remain three m_C^R -dependent factors in eq A11, namely m_C^R , E_1 , and E_2 , when r , β' , and f_1 (or f_s) are held constant. Inserting eq A11 into eq A14 and taking the derivative yields

$$\begin{aligned} 0 &= \left\{ \beta' e^{-1} + m_C^R \beta' e^{-1} 2(1-r)L_B \frac{\partial S}{\partial\lambda} \frac{K}{2} \left(\frac{1+f_s}{2} \right)^{1/2} \times \right. \\ &\quad \left. \frac{1}{(m_C^R)^{1/2}} + m_C^R \beta' e^{-1} (1-r)L_B \frac{K^2}{4} m_1 (1-r) \frac{1}{\lambda} \left(-\frac{1}{\lambda} \frac{\partial S}{\partial\lambda} + \frac{\partial^2 S}{\partial\lambda^2} \right) \times \right. \\ &\quad \left. \frac{K}{2} \left(\frac{1+f_s}{2} \right)^{1/2} \frac{1}{(m_C^R)^{1/2}} + m_C^R \beta' e^{-1} (1-r)L_B \frac{K^2}{4} f_1 \frac{1}{\lambda} \frac{\partial S}{\partial\lambda} \right\} E_1 E_2 E_3 \end{aligned} \quad (\text{A18})$$

After making use of eqs A9, 6, A8, and A13, dividing by r , and rearranging somewhat, one can solve for $1-r$ in terms of m_C^R , λ , f_1 , and f_s , all of which depend on $1-r$. The final result is

$$r = 1 - \frac{1}{(m_C^R)^{1/2} L_B K \left(\frac{1+f_s}{2} \right)^{1/2} \left\{ -\frac{\partial S}{\partial\lambda} \left(1 + \frac{1}{4} \left(\frac{f_1}{1+f_s} \right) \right) - \frac{1}{4} \left(\frac{f_1}{1+f_s} \right) \lambda \frac{\partial^2 S}{\partial\lambda^2} \right\}} \quad (\text{A19})$$

For convenience, we denote the total concentration of small ions, including both uncondensed counterions and coions, at R by

$$m_{\text{si}}^R \equiv m_C^R + m_s^R = m_1(1-r) + 2m_s^R \quad (\text{A20})$$

We note further that $1+f_s = (m_{\text{si}}^R/m_C^R)$ and $f_1/(1+f_s) = m_1(1$

— $r)/m_{\text{si}}^{\text{R}}$. With these substitutions, eq A25 can be written in the form of eq 9 in the text.

References and Notes

- (1) Raspaud, E.; da Conceicao, M.; Livolant, M. *Phys. Rev. Lett.* **2000**, *84*, 2533.
- (2) Manning, G. S. *J. Chem. Phys.* **1969**, *51*, 924.
- (3) Oosawa, F. *Polyelectrolytes*; Marcel Dekker: New York, 1971.
- (4) Manning, G. S. *Biophys. Chem.* **1977**, *7*, 95.
- (5) Manning, G. S. *Q. Rev. Biophys.* **1978**, *11*, 179.
- (6) Manning, G. S.; Ray, J. J. *Biomolec. Struct. Dyn.* **1998**, *33*, 191.
- (7) Hansen, P. L.; Podgornik, R.; Parsegian, V. A. *Phys. Rev. E* **2001**, *64*, 64.
- (8) Fuoss, R.; Katchalski, A.; Lifson, S. *Proc. Natl. Acad. Sci. USA* **1951**, *37*, 579.
- (9) Lifson, S.; Katchalski, A. *J. Polym. Sci.* **1954**, *13*, 43.
- (10) Anderson, C. F.; Record, M. T., Jr. *Annu. Rev. Phys. Chem.* **1982**, *33*, 191.
- (11) Klein, J. W.; Ware, B. R. *J. Chem. Phys.* **1984**, *80*, 1334.
- (12) Heath, P. J.; Schurr, J. M. *Macromolecules* **1992**, *25*, 4149.
- (13) Rhee, K. W.; Ware, B. R. *J. Chem. Phys.* **1983**, *78*, 3349.
- (14) Yen, W. S.; Rhee, K. W.; Ware, B. R. *J. Phys. Chem.* **1983**, *87*, 2148.
- (15) Ma, C.; Bloomfield, V. A. *Biopolymers* **1995**, *35*, 211.
- (16) Schurr, J. M.; Schmitz, K. S. *Annu. Rev. Phys. Chem.* **1986**, *37*, 271.
- (17) Klein, B. K.; Anderson, C. F.; Record, M. T., Jr. *Biopolymers* **1981**, *20*, 2263.
- (18) Stigter, D. *Biophys. J.* **1995**, *69*, 380.
- (19) Schurr, J. M.; Fujimoto, B. S. *Biophys. Chem.* **2002**, *101–102*, 425.
- (20) Manning, G. S. *Macromolecules* **1999**, *34*, 4650.
- (21) Naimushin, A.; Fujimoto, B. S.; Schurr, J. M. *Macromolecules* **1999**, *32*, 8210.
- (22) Katchalsky, A. *Pure Appl. Chem.* **1971**, *26*, 327.
- (23) Alfrey, T., Jr.; Berg, P. W.; Morawetz, H. *J. Polym. Sci.* **1951**, *7*, 543.
- (24) Imai, N.; Mandel, M. *Macromolecules* **1982**, *15*, 1562.